Chemical Engineering Journal 479 (2024) 147205



Contents lists available at ScienceDirect

Chemical Engineering Journal

journal homepage: www.elsevier.com/locate/cej





Electrified steam methane reforming of biogas for sustainable syngas manufacturing and next-generation of plant design: A pilot plant study

Thomas N. From [a,b], Behzad Partoon [a], Marené Rautenbach [b], Martin Østberg [b], Anders Bentien [a], Kim Aasberg-Petersen [b], Peter M. Mortensen [b,*]

[a] Department of Biological and Chemical Engineering, Aarhus University, Hangøvej 2, 8200 Aarhus N, Denmark
[b] Topsoe A/S, 2800 Kongens Lyngby, Denmark

ARTICLE INFO

Keywords:
Biogas
Steam methane reforming
Electrification
Sustainable chemicals and fuels
Renewable energy
Industrial catalysis

ABSTRACT

Electrification of the traditional steam methane reforming (SMR) technology for syngas manufacturing has a significant CO_2 reduction potential and make it more feasible to operate in combination with carbon capture/utilization, especially if renewable electricity is used. This pilot plant study demonstrates the first operational experience with industrial-scale electrified steam methane reforming (eSMR) technology using biogas as sustainable carbon feedstock. Across an operating envelope spanning from combinations of 5 to 20 bar_g and 750 °C to 1000 °C, the eSMR produces syngas as expected from thermodynamics. However, without the thermal restrictions inherent in the SMR design, the eSMR can achieve higher temperatures, enables fast transient operation, with high stability and control, thereby increasing the overall performance and design flexibility. Initial thermal responses of the eSMR were tested, demonstrating fast start-up from an idle state to operating conditions, within 2.6 h, including heating from 630 °C to 900 °C. Furthermore, dynamic temperature control was also demonstrated with heating rates up to 330 °C/h. Experimental energy efficiency of the pilot reactor was quantified between 72 % and 80 %, with the residual being heat loss to the surroundings due to the relatively small scale. With further scale-up to ≥1 MW reactor capacity, efficiencies of ≥99 % are predicted with a specific electrical energy consumption of 1.0 kWh/Nm^3 H_2. Overall, the efficiency and operational flexibility are improved due to the direct electrical heating of the catalytic system. Combined with biogas as feedstock, this paves the way for attractive and competitive plant designs for sustainable and renewable production of chemicals and fuels.

1. Introduction

The global transition to a low-carbon and sustainable production requires purposeful, transformative, and non-marginal technological, systemic, and socio-behavioral changes that disrupt existing development trends. In line with this perspective, the European Union (EU) has put forward "Fit for 55" package targeting a 55 % reduction of GHG emissions from EU countries by 2030. The proposed package targets legislation in different areas, aiming to move towards a more sustainable world [1]. Low-carbon energy systems are expected to depend increasingly on electrification, where electricity is produced with low global greenhouse gas (GHG) emissions, such as wind and solar power [2]. However not all industries, in particular shipping and aviation, will be able to use electricity as a direct propulsion source, and therefore, sustainable fuels such as hydrogen and hydrogen derivatives (e.g., ammonia, methanol, synthetic fuels) will be a requirement to meet the targets [2].

Despite green hydrogen (generated from a renewable energy source) is considered as a central element in decarbonizing the global chemical and fuel production, 96 % of the global hydrogen production is still derived from fossil fuels, (grey hydrogen), where natural gas counts for 48 %, heavy oil and naphtha for 30 %, and coal for 18 % of the global feed stock. Only 4 % of the global hydrogen production comes presently from electrolysis, whereof only 25 % is directly based on renewable electricity [3]. The steam methane reforming process is the most widespread route for producing hydrogen from natural gas, and it is expected to remain the dominant process for large-scale hydrogen production because of its favorable economics and existing infrastructure [4,5]. In that perspective, blue hydrogen has an increasing interest, as its origin is based on fossil fuel, but where some or nearly all the CO_2

* Corresponding author.
E-mail address: pmor@topsoe.com (P.M. Mortensen).

https://doi.org/10.1016/j.cej.2023.147205
Received 14 August 2023; Received in revised form 3 November 2023; Accepted 6 November 2023
Available online 10 November 2023
1385-8947/© 2023 The Authors. Published by Elsevier B.V. This is an open access article under the CC BY-NC license (http://creativecommons.org/licenses/by-nc/4.0/).

emissions associated with its production are captured and sequestered. Existing technologies like fired tubular reforming (SMR) and auto-thermal reforming (ATR) in combinations with carbon capture have therefore already been proposed and implemented to produce blue hydrogen [5,6].

In industrial fired tubular reforming plants (SMR), natural gas is mixed with steam, and where applicable CO_2, and converted into hydrogen and carbon oxides; referred to as synthesis gas (syngas). The steam methane reforming process is governed mainly by the thermodynamically independent steam methane reforming and water gas shift reactions shown in Reaction (1) and (2), respectively. In the case of CO_2-reforming, the water gas shift reaction (Reaction (2) plays an increased role. Combining Reactions (1) and (2) gives the dry methane reforming reaction (Reaction (3). Despite many combination possibilities, the overall reaction scheme is for all cases strongly endothermic.

$$CH_4(g) + H_2O(g) \rightleftarrows 3\,H_2 + CO(g) \quad (\Delta H_r^\circ = 206 \frac{kJ}{mol}) \tag{1}$$

$$CO\,(g) + H_2O(g) \rightleftarrows CO_2(g) + H_2(g) \quad (\Delta H_r^\circ = -41 \frac{kJ}{mol}) \tag{2}$$

$$CH_4(g) + CO_2(g) \rightleftarrows 2\,H_2(g) + 2CO(g) \quad (\Delta H_r^\circ = 247 \frac{kJ}{mol}) \tag{3}$$

Syngas as an intermediate facilitates a production platform of large-scale chemicals including ammonia, methanol, and liquid fuels, among others. Configuration of these chemical production plants is favored by operating the SMR plants at high pressure. However, following the Le Chatelier's principle, this limits the conversion of the reforming reaction, and in order to compensate for this, higher temperatures are required to drive the endothermic reforming towards sufficient methane conversion [7].

The industrial (grey) SMR process has a significant CO_2 footprint, as approximately 8.6–9.3 tons of CO_2 are produced per ton H_2, where 17–41 % is a direct result of combustion of fuel and off-gas to provide the required heat for the syngas production [5,8–10]. Typically, the fired reformer is the largest, most complex, and most expensive unit operation in syngas production. It consists of catalyst loaded in a large number of high-alloy steel tubes that are placed in a large furnace, heated by combustion of fossil fuels and off-gases from the process. This configuration allows for around 50 % of the supplied heat to be directly transferred to the reforming reaction in the catalyst bed, while the rest leaves as latent heat in the above 1000 °C hot flue gas [11]. The combustion temperature of the burners must therefore be significantly above the reaction temperature in order to generate the required inward heat flux [7,10]. To achieve a high energy efficiency of a SMR plant configuration, an integrated flue gas waste heat sections is a requirement, where the efficiency can be increased up to ca. 95 % if production of excess steam is included [7]. Performance of industrial SMR plants is typically limited by the heat transfers across the fired reformer. Combining low thermal conductivity with strong endothermic steam methane reforming creates a steep temperature gradient across the catalyst bed, increasing the risk of hot spots, and cause thermal stress detrimental to reactor lifetime. Typical economic and practical operation of industrial SMR plant is therefore around 15–30 bar_g and 850–920 °C limited by material constraints [7,10,12,13]. Large furnace chambers, compression of gas, and extensive heat recovery favor operation at large scale, restricting economic operation to large centralized SMR plants [7,11]. In addition, during start-up, flowrates and heat inputs are gradually increased over several days before reaching steady state operation as the fired section and catalytic section of the SMR always needs to be balanced. Consequently, industrial SMR plants perform best when operated under steady state operation, as they are not suited for dynamic change in temperature, pressure, or load [7,10–13].

For decades, the low thermal conductivity of fired reformers has been a topic of research. This includes investigation into materials and catalysts with higher conductivity [14–17], shorter characteristic length scales for heat transfer [17–19], different reactor concepts [20,21], reduced temperature by shifting the equilibrium [22,23], or heating of magnetic catalysts by induction [24–26]. Recently, Wismann et al. [10] successfully integrated an electrically heated catalytic structure with the steam methane reforming reaction. The integrated solution gave an intimate contact between the electric heat source and the catalyst, thereby supplying energy directly to the catalytic active site with practically no temperature difference from heat surface to catalytic site. This integration overcomes the heat transfer limitations known from industrial SMR plants. Having a uniform supply of heat to the process also ensures that gas composition is kept close to equilibrium throughout the entire catalytic length, reducing reactor volume and leading to a higher utilization of the catalyst material. Numerous examples of electrified reforming processes have been reported, which involve the use of structured catalysts. These include induction heating of ferromagnetic catalyst [24,25], microwave heating of a structured Ni/SiC catalyst [27,28] or ohmic heating [29,30]. Fast temporal response and dynamic operation is achievable as a result of the electrical heating, contrary to industrial SMR plant where low heating rates and steady state operation are required to avoid thermal stress or formation of hotspots [12,13]. These features are especially interesting in a world where the need for more flexible technologies is in high demand for dynamic operations.

The electrified steam methane reforming (eSMR) technology effectively removes the need for a combustion section in the steam methane reforming scheme, thereby eliminating the directly associated CO_2 emissions, assuming use of renewable electrical power. If, in addition, biogas or SNG, from renewable sources, is introduced as carbon feedstock, the process has a great potential for sustainable and renewable production of syngas. Biogas consist of biogenic carbon with a CH_4 and CO_2 concentrations between 50 and 75 mol% and 25–50 mol%, respectively [31]. This high concentration of CO_2 in biogas is within the range already applied for SMR feeds in industrial scale [32]. Biogas production is also a common and mature process that has gained focus for its potential role as sustainable carbon source and waste handling. In a biogas plant, biomass waste and manure from primarily agriculture are used in an anaerobic digester (AD) operating under mild conditions (35–60 °C) to produce biogas and residue streams. The residue is rich in minerals and can work as an excellent fertilizer, and is often returned to the agriculture sector [33–35]. However, biogas contains sulfur compounds mainly in the form of H_2S (1000–2000 ppm) that need to be removed to enable catalytic steam methane reforming of biogas, as sulfur contamination, even in the range of 1–10 ppb, can lead to deactivation of the Ni-based catalyst [36,37]. Nonetheless, the work of Dannesboe et al. [37] proved, in full scale with 1000 h operation, that deep sulfur removal of biogas for catalytic reforming on a nickel based catalyst is possible, using combination of well-known technologies like a biotrickling filter, activated carbon, and sulfur guard.

Biogas production needs integration with a downstream process to convert the produced gas into a valuable end-product. The simplest use is for energy production (electricity and/or heat) by a gas engine, but the relative low heating value (LHV) of raw biogas of 16–28 MJ/m^3 makes it less sufficient as fuel compared to natural gas with LHV of around 36 MJ/m^3 [38]. This is due to the high CO_2 content in the biogas. Alternatively, biogas can be upgraded to bio-methane as a substitute for natural gas. This is typically done today by separating the CO_2 by an energy intensive gas cleaning step such as amine or water scrubbers as well as pressure swing adsorption [36]. The residual byproduct of CO_2 is typically emitted to the atmosphere, resulting in large amounts of carbon being wasted. This emission is technically green, but it is still undesired because CO_2 can be used as a building block for sustainable fuels and chemicals production [39–42]. In 2021, Europe had almost 18,000 biogas production plants, where 97 % of them used the biogas for local heat and power generation. Only the remaining 3 % of the plants upgraded biogas to biomethane to be injected into the natural gas grid

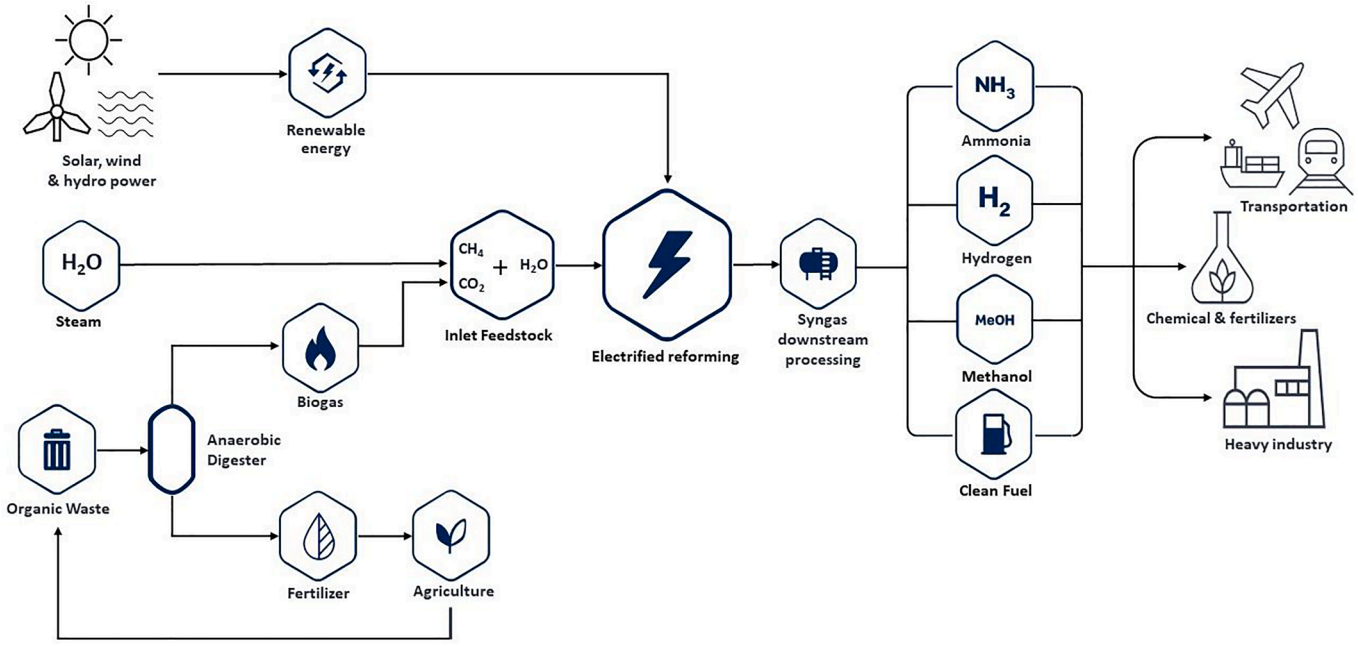


Fig. 1. Flow diagram of biomass to sustainable chemicals and fuels utilizing the electrified steam methane reformer (eSMR).

[43]. This presents an opportunity for valorization of the biogenic carbon to more sustainable products, which prospectively could substitute fossil carbon in other sectors. With the present attention to emerging Power-to-X (PtX) technologies, this expands the possibilities beyond using green hydrogen (e.g. from electrolysis) either for direct methanation of biogas over a high-surface-area nickel catalyst converting CO_2 to CH_4 (biomethane) [37,42,44] or converting captured CO_2 to valuable chemicals or fuels [43,45].

This work focuses on the combination of biogas and the eSMR technology, which provides an alternative PtX route for sustainable chemical and fuel productions. This is achieved by utilizing a combination of renewable electricity and sustainable carbon feedstock to produce syngas, enabling sustainable production of green fuels and chemicals. In practice, this configuration allows for almost zero-emission chemical plant with high carbon utilization. This new configuration demonstrates the potential for disruption of the chemical industry towards a more sustainable approach. This scheme is summarized in Fig. 1.

2. Material and methods

Experimental work was commenced at the first-of-a-kind pilot-scale eSMR unit on *Topsoe eREACT*™ technology. The eSMR unit is installed in the Power-to-X process hall of the biogas research facility located at the Aarhus University (AU), Viborg campus, Denmark. The unit receives a raw biogas feedstock from a small industrial scale biogas production plant having a 1200 m^3 anaerobic digester [37]. The eSMR unit consists of a pre-treatment section, steam generator, prereformer, eSMR, waste heat boiler (WHB), condensate separation and utilities sections, as shown in Fig. 2A together with pictures from the installation.

The raw biogas mostly consists of methane (50–75 mol%) and carbon dioxide (25–50 mol%) with small impurities like nitrogen (up to 2 mol %) and hydrogen sulfide (~1000 to 2000 ppm), and it is saturated with water at ambient conditions (20–60 $mbar_g$) [46]. In order to protect the catalyst in the downstream reforming section, the hydrogen sulfide and any other potential sulfur compounds are removed from the biogas. The biogas pretreatment was done in the same setup used in previous work of Dannesboe et al. [36], which consists of low-pressure/low-temperature sulfur guards for bulk removal of H_2S, a biogas compressor, and a high-pressure/high-temperature sulfur guard for removing possible remaining H_2S and other sulfur compounds. The biogas is pressurized to the process pressure (10–25 bar_g) using a two-stage diaphragm compressor, MV 4722IIK, from *Sera* (Fig. 2B). The steam generator consists of a water pump, high-pressure electric boiler, and a steam superheater. In the steam generation section, demineralized water is pumped to a steam generator where it is evaporated under pressure up to 60 bar_g. The generated steam is subsequently superheated. The superheated steam and desulfurized biogas are mixed forming the process gas which is preheated to 350–400 °C. Hereafter, the process gas enters the prereformer, which contains a commercial nickel-based catalyst, AR-401 from *Topsoe*. Prereforming is used to convert higher hydrocarbons if present in the process gas [32,47]. The process gas then enters the eSMR reactor shown in Fig. 2C. The reactor includes an alumina-based refractory lining encapsulate the catalyst zone from the surrounding reactor shell, thereby keeping a low temperature on the reactor pressure shell. The reactor is loaded with a Topsoe industrial eREACT™ catalyst system constituting a direct electrical heated catalytic structure with nickel as the active material. The reactor is operated using electric heating, similar to previous work on the analogous bench-scale design [10,12,48]. Electricity is supplied from a N8951A Power Supply Unit from *Agilent Technologies*. Reactor temperature was measured with K-type thermocouples positioned at the catalyst exit.

The eSMR reactor produces syngas at exit temperatures of 750–1000 °C, which is then cooled, first down to 100–130 °C in an waste heat boiler shown in Fig. 2D [49], and then further to ≤40 °C in a water-cooled plate heat exchanger. Condensate is subsequently removed in a high-pressure separator. The dry syngas is analyzed by a gas chromatograph (GC) (7890B, *Agilent Technologies*) for CO, CO_2, CH_4, N_2, and H_2. Higher hydrocarbons up to C6 can also be analyzed if present. The GC is equipped with two columns (MS5A and Rt-Q-BOND), thermal conductivity (TCD) – and flame ionization detectors (FID). System pressure is controlled using an equilibar back pressure regulator placed after the HP separator. After depressurization, the syngas is flared to avoid releasing CO, unconverted CH_4, and H_2 into the environment. The condensate is after depressuring passing a low pressure condensator separating released gas from condensate. The released gas is re-mixed with the main gas stream after depressuring.

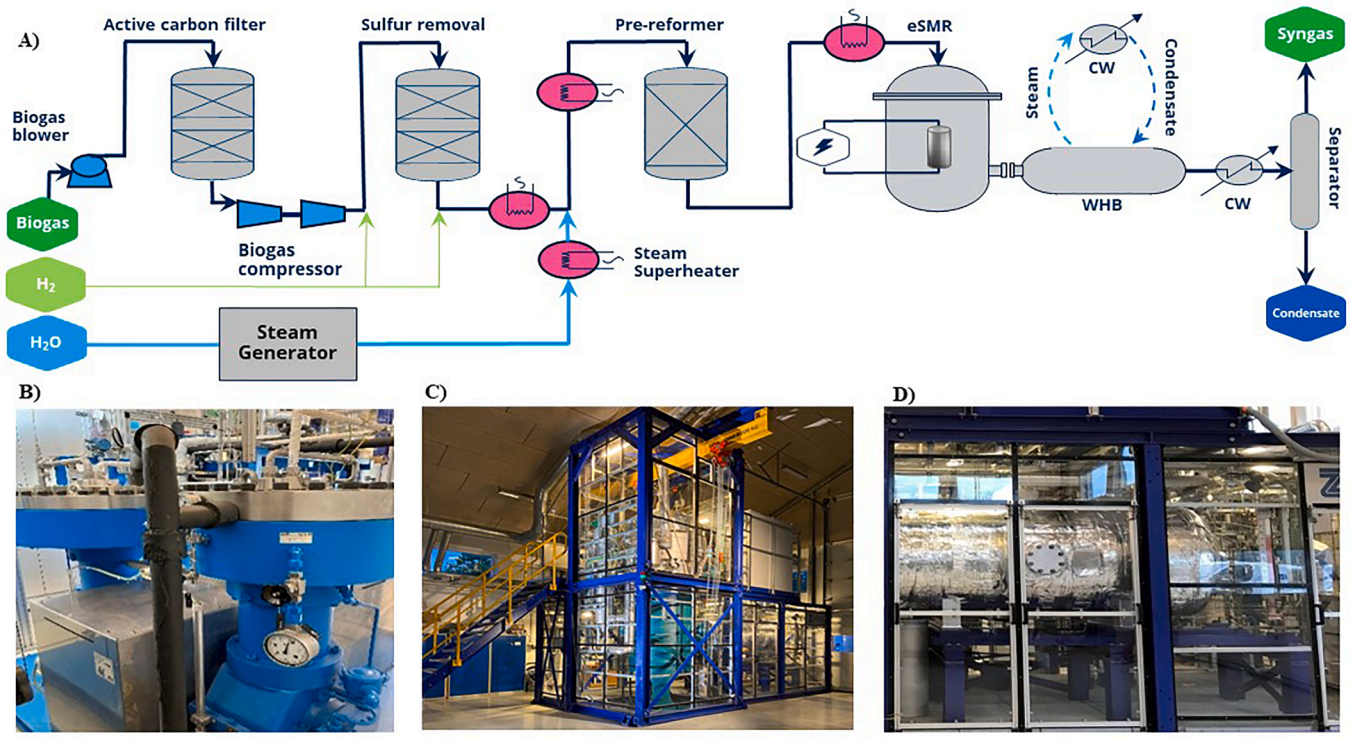


Fig. 2. (A) Simplified block diagram of the eSMR setup; (B) compressor section; (C) the electrified steam methane reformer (eSMR); (D) the waste heat boiler.

3. Results and discussion

To enable an industrial relevant evaluation of the performance in the pilot scale, test was made with respect to; thermal response, stability, verifying thermodynamic performance, operation envelope, energy efficiency, and energy consumption as well as investigate the synergy of using biogas as a sustainable carbon source for syngas production. The data were compared with industrial SMR performances and, in the end, a potential process design including the eSMR technology was compared with an industrial SMR plant design for production of syngas. The total tested operating regime covers 750 °C–1000 °C, 3–20 bar_g and steam-to-carbon ratio (S/C) 2.1 to 2.7. The pilot plant data presented in this work covers initial operation close to 2000 h.

3.1. Start-up of electrified steam methane reactor

The pilot scale eSMR reactor was tested with a start-up procedure from idle condition to stationary operation including steam and subsequently biogas introduction, and temperature increase using full automation control based on electrical heating. Fig. 3 shows the temperature

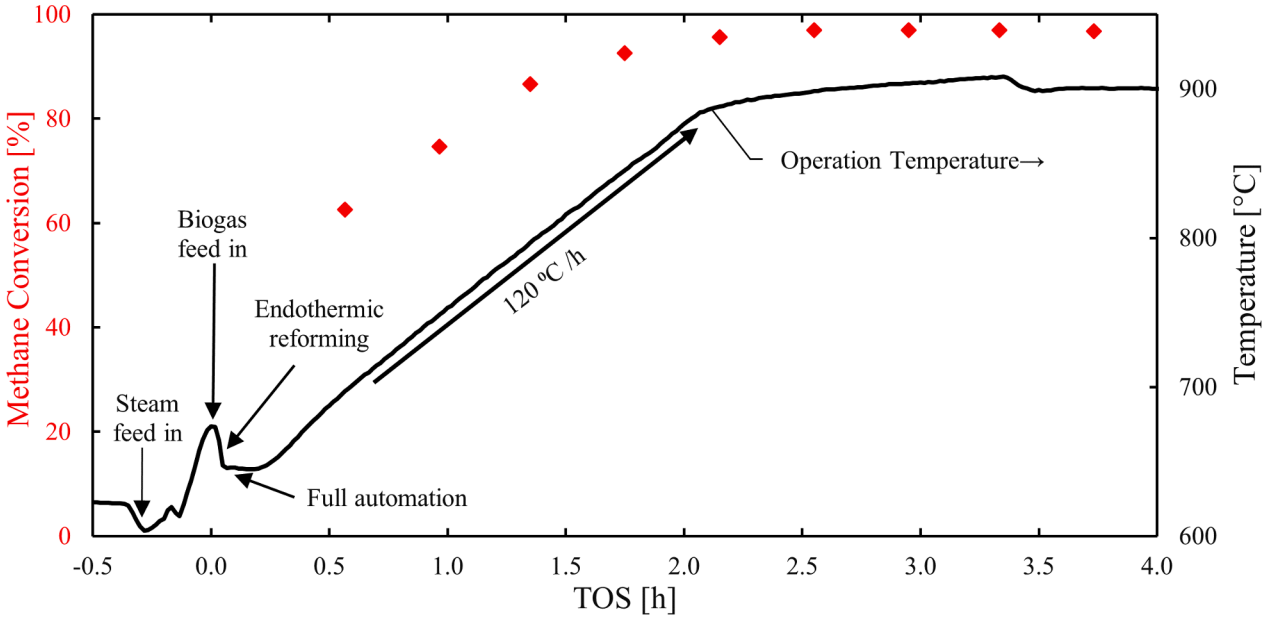


Fig. 3. Start-up of the industrial representative pilot scale eSMR reactor from idle state at 645 °C to operation at 900 °C. Conditions: Inlet temperature 400 °C, pressure 10 bar_g, and steam-to-carbon ratio 2.7.

development for the eSMR reactor as a function of time on stream (TOS), covering feed introduction and thermal heating from 645 °C to 900 °C, showing the transient from idle state to stationary operation. Experimental data of methane conversion (calculated from the carbon balance) is included in Fig. 3.

In Fig. 3, steam was added at TOS = −0.3 h to the nitrogen flow, which results in a temperature drop due to higher heat capacity and flow rate, this was subsequently counteracted by increasing the power. The biogas was added at TOS = 0 where a second temperature drop occurred due to the endothermic reforming of biogas. The temperature control of the eSMR reactor was switched to auto control at 645 °C after 4 min (TOS = 0.08 h) with 900 °C as final set point and having a heating rate of 120 °C/h. The exit temperature began to increase after 8 min in auto control, and the eSMR reactor reached a fast and stable heating rate of 120 °C/h at TOS = 0.7 h, controlling with an average deviation of 5.2 °C from the set point value during ramping (1 min sampling frequency). The methane conversion followed the increasing temperature until reaching a steady state conversion of 97 % after 2.3 h, which was in thermodynamic equilibrium with respect to the reforming reactions (1) and (2). In this start-up experiment, the eSMR reactor reached the set point temperature at 900 °C after 2.6 h. The time between initializing auto control for the temperature increasement and reaching the desired heating rate was affected by heat losses from the pilot plant reactor beside the endothermic reforming. This delays the time before reaching a stable regulation of the system. It is worth mentioning that the initial parameters used in the PID feedback-control in Fig. 3 were selected for optimal steady state operation. Although, the presented start-up time is much faster than conventional fired SMR, further PID tuning towards fast dynamic changes could increase the heating rate further to obtain even faster thermal responses. The total time of 2.6 h is therefore an initial result and could be further optimized.

3.2. Exploration of operating envelope

Industrial SMR is limited in performance due to low thermal conductivity across the reactor wall and catalyst bed. Temperature difference up to 100 °C between the reactor wall and the catalytic center are reported for packed-bed steam-methane reformers [13,50–52]. Operating temperatures are therefore limited as well as steady state operation due to material constraints. In that perspective, the agility of operation the eSMR technology at industrial representative scale was investigated at different exit temperatures. In Fig. 4, the power load is shown as function of TOS while varying the exit temperature from 900 °C to 750 °C to 1000 °C. The initial exit temperature of 900 °C was used as a reference point for the power load at 100 %. The initial set point was changed to 750 °C at TOS = 0, and the new exit temperature was reached after 10 min having a small undershoot of 19 °C but stable again after 70 min with a deviation of 0.8 °C based on 1 min sampling frequency. The temperature drop corresponds to a power cut of 49 % with a cooling rate of 1000 °C/h and demonstrates a fast thermal response and accurate control of the electrified system. The fast-cooling rate is facilitated by direct cooling from the endothermic reaction environment. The exit temperature was then increased in 50 °C intervals where heating rates up to 330 °C/h were demonstrated in this current configuration. In between step changes, the exit temperature was kept at steady state conditions for 1–2 h to collect data and investigate stability. In all step changes, the temperature overshoot was not more than 5 °C from the set point value with a maximum deviation of 1.3 °C, and a new steady state condition reached within 30 min. However, since exit temperature of 1000 °C was new ground of the steam methane reforming, a lower heating rate of 52 °C/h was selected resulting in steady state operation after 60 min. The expansion of the temperature operating regime up to 1000 °C improves the methane conversion and thereby reduces the methane slip out of the eSMR reactor, which will increase the feed utilization in an eSMR configuration.

The exit temperature control system of the eSMR reactor is a direct feedback-control of power input to the eSMR reactor controlling the desired exit temperature. This is found to be very efficient when combining the intimate contact between the heat source and the catalyst in the eSMR reactor, having a fast power response occurring on a millisecond level, which enables fast and precise temperature changes. As in previous section, Fig. 4 had a PID feedback control system optimal for steady state operation and therefore temperature response could be further optimized. The eSMR reactor technology has already show great opportunities for dynamic operation, suitable to address the intermittent nature of different sources of renewable electricity used for P2X

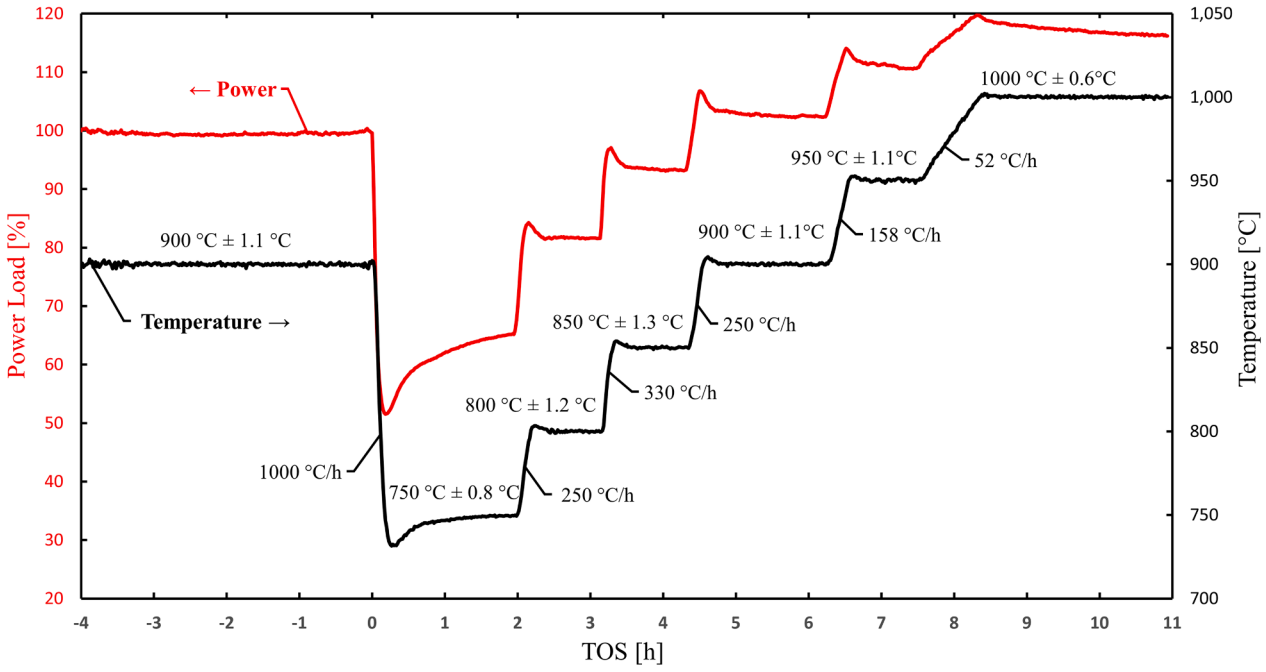


Fig. 4. Temperature and power profiles. Conditions: 16 bar_g and a steam-to-carbon at 2–2.2 [-]. Initial power load of 100% is relative to the base case condition operation at 900 °C.

operation.

3.2.1. Catalytic stability test

The eREACT™ catalyst system has consistently displayed stable performance, despite exposure to various operating scenarios, including multiple start-ups and shutdowns, transient operation, as well as high temperature. This is shown in Table 1, which compares two steady-state operating points, at similar conditions, with 1050 h of operation in between. The variation in S/C and CH_4 conversion can be attributed to the fluctuating methane concentration of biogas, a common occurrence in biogas reforming. Methane conversion was according to thermodynamic principles, and without any sign of catalyst deactivation.

3.3. Energy efficiency and scale up production

The energy efficiency of the eSMR reactor was tested at different biogas flow rates at inlet temperature of 400 °C, exit temperature of 900 °C, pressure at 10 bar_g, and S/C ratio between 2 and 2.2. The energy efficiencies, based on enthalpy of reaction, were calculated at four different low flow ranges varying from 15 Nm^3/h to 27 Nm^3/h, resulting in an efficiency of 72 % to 80 % for low capacities, indicated in Fig. 5. The remaining energy is heat loss, primary to the surroundings and minor to electrical parts. Low capacities were investigated to give a larger description of the energy efficiency development, which subsequently was used to derive a simplified energy efficiency model of the eSMR reactor derived from the basic energy balance of the reactor for extrapolation to higher capacities and industrial comparison. Fig. 5 summarizes experimental calculated efficiencies as a function of capacity as well as the energy efficiency and energy consumption model. Using the derived model, expected energy consumption was calculated based on equilibrated gas for hydrogen production at S/C 1.8, inlet temperature 400 °C, exit temperature 920 °C and pressure 30 bar_g. Natural gas operation was modelled in the energy consumption for industrial comparison. A detailed description of the model implementation of the energy efficiency and energy consumption is included in Supporting Information.

Based on simple modelling, Fig. 5 shows as expected increased efficiency of the eSMR reactor as capacity is increased and extrapolates to above 99 % at capacities above 1 MW. The model assumes that the principal loss mechanism of the eSMR is heat loss to the surroundings through the surface area of the reactor. Consequently, when scaling up the capacity of the eSMR, the surface area heat loss in the end becomes relatively low. For reference, an industrial hydrogen reforming plant at 1 MW capacity based on the eSMR technology could produce in the order of 1000 Nm^3 H_2/h with an energy efficiency of 99 %.

The energy consumption curve in Fig. 5 represents the specific electrical energy consumption of the eSMR and translates into the enthalpy of reaction for the steam methane reforming reaction ($CH_4 + H_2O$). The energy consumption is consequently calculated per Nm^3 syngas (combined $H_2 + CO$), however, in case of hydrogen production, CO would be shifted to H_2 through a WGS reactor downstream the eSMR and thereby can be assumed equivalent to H_2 [7], resulting in a 1.0 kWh/ Nm^3 H_2 at a capacity above 1 MW completely covered by (renewable) electricity. Adding the natural gas feedstock, the specific net energy consumption of an eSMR based process for hydrogen production is 3.6 kWh/Nm^3 H_2 as there is an additional 2.6 kWh/Nm^3 H_2 due to the LHV equivalent of the natural gas feed. For comparison with other industrial hydrogen processes, a classical SMR plant has a specific net energy consumption of 4.2 kWh/Nm^3 H_2 all being LHV equivalent of natural gas feed [53], 17 % higher than the eSMR based layout. The lower energy consumption is a consequence of the improved thermal contact in the eSMR reactor resulting in higher energy efficiency and better feedstock utilization compared to the SMR counterpart. In addition, these numbers also display that the eSMR uses 38 % less natural gas feedstock compared to SMR for production of the same quantity of hydrogen. This is a result of the high temperature service at 900–1000 °C of the eSMR allowing for high feedstock utilization and consequently obtaining near stoichiometric consumption figures on the feedstock side. When used for e.g. blue hydrogen application, this results in a reduced amount of CO_2 that needs to be handled, compressed and sequestrated.

Table 1
Evaluation of the stability of the eREACT™ catalyst system after 1050 h of operation at industrially representative reforming conditions.

	Time 1	Time 2
TOS [h]	485	1535
S/C [-]	2.1 ± 0.1	2.1 ± 0.1
Temperature [°C]	950	950
Pressure [Bar_g]	20	20
CH_4 Conversion [%]	94 ± 1	94 ± 1

As alternative to syngas (or hydrogen) production by steam reforming, the specific net electrical energy consumption in water electrolysis systems are in the range 3.7–6.6 kWh/Nm^3 H_2, depending on choice of electrolysis technology and system integration [54]. Comparing the electrical demand in the water electrolysis systems with the total energy demand in the eSMR solution of 3.6 kWh/Nm^3 H_2, eSMR is lower than best in class electrolysis solution. More markedly though, when comparing specific electrical energy consumption of eSMR to electrolysis solutions, eSMR is 75–85 % lower. The markedly lower electrical energy consumption in the eSMR reactor is firstly due to the lower heat of reaction and secondly due to the very high energy efficiency inherent in the eSMR reactor. Syngas (or hydrogen) production consequently scales better with eSMR technology relative to electrolysis technology relative to available (renewable) electricity supply.

3.4. Industrial perspective

The presented experimental work demonstrates how the eSMR technology allows for agile operation, precise process control, and syngas production according to thermodynamics. By extrapolating the design of the current unit shown in Fig. 2 to an industrial counterpart, it is demonstrated that a simplified process configuration is achievable with the eSMR technology. This simplification is illustrated in Fig. 6, which schematically shows an industrial fired SMR (A) compared with an electrically driven eSMR (B). The central difference between the eSMR and SMR design is the replacement of fossil fuel (natural gas) and off-gas with renewable electricity to provide the necessary heat to drive the reforming reactions, which remove the hottest and largest stream from the plant. This completely removes the furnace section and subsequently several additional unit operations, including flue gas fan, combustion air blower, flue gas stack, heat exchangers for heat recovery of the hot flue gas as well as the utilization of combustion air.

Where the SMR plant design is configured around the flue gas waste heat section to facilitate process pre-heating, the eSMR plant design has a higher degree of freedom. In this layout pre-heating can be done by any suitable technology according to best practice. Steam pre-heaters can be used if excess steam is available in the steam balance, electrical heaters or firring with H_2 can be used for separate process heaters. In case of excess fuel gas in the plant design, a fired heater can be considered. The latter is however least preferred due to an associated CO_2 emission. With increasing operation temperature in the eSMR design, tested up to 1000 °C in this study, the methane conversion will increase accordingly and thereby reduce the methane slip. Together with the absence of the furnace section, this enables better feedstock utilization. In that perspective, the eSMR design allows for several attractive process configurations with natural gas or biogas.

This could e.g. be production of blue hydrogen from natural gas with complete carbon capture due to the absence of associated flue gas [5]. For comparison, hydrogen production in traditional SMR layout result in a carbon intensity of 9.2 kg CO_2/kg H_2 without carbon capture, and

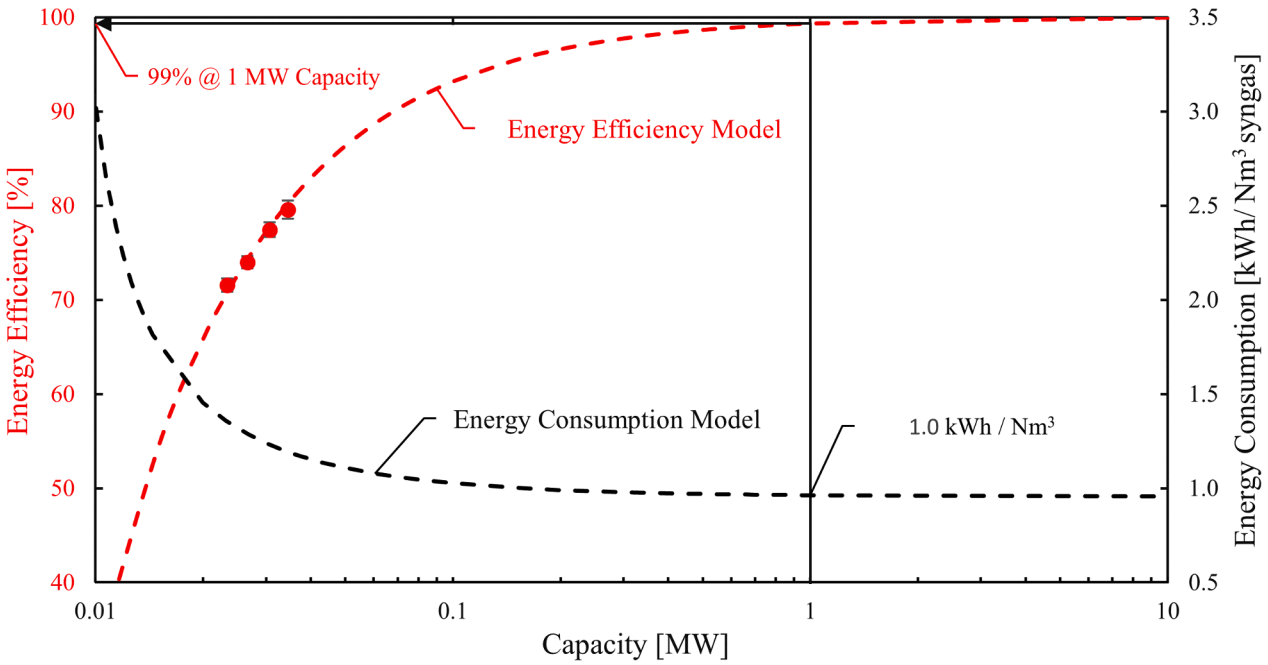


Fig. 5. Energy efficiency and energy consumption as a function of capacity of the eSMR reactor. The Experimental data (dots) were carried out at biogas flow ranges from 15 Nm^3/h to 27 Nm^3/h, inlet temperature of 400 °C, exit temperature of 900 °C, pressure at 10 bar_g and steam-to-carbon ratio between 2 and 2.2. Low capacities were investigated to give a larger description of the energy efficiency development. The energy consumption model for hydrogen production predicted with an inlet temperature of 400 °C, exit temperature of 920 °C, and pressure at 30 bar_g and steam-to-carbon ratio 1.8.

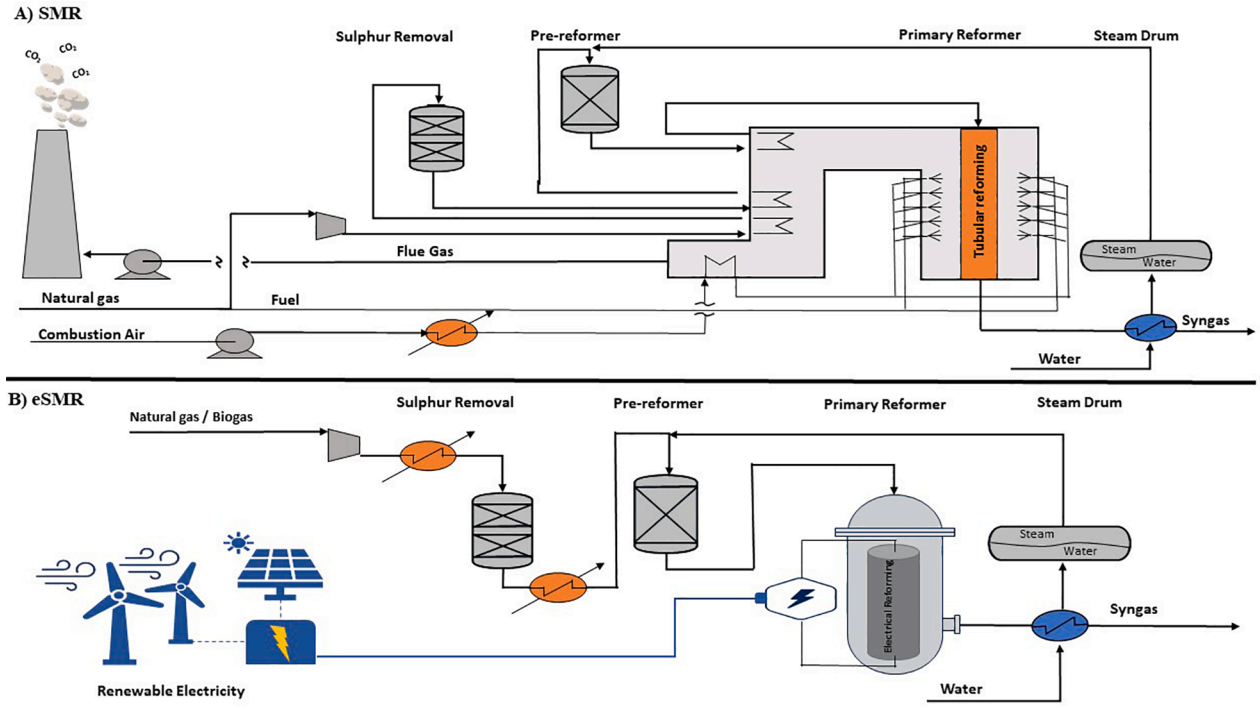


Fig. 6. Flowsheet of A) Industrial fired SMR design utilizing natural gas as fuel and B) potential eSMR design utilizing renewable electricity as fuel.

about 3.6 kg CO_2/kg H_2 with carbon capture from the process side only. The eSMR configuration allows carbon intensity to be lowered to approximately 5.7 kg CO_2/kg H_2 without carbon capture corresponding to process stoichiometry, and less than 0.1 kg CO_2/kg H_2 with carbon capture. This makes it an excellent option for producing blue hydrogen from natural gas [53].

Additionally, the eSMR configuration enables dynamic and feasible operation of different reactor sizes, which promote delocalization designs [10]. This is especially important for eSMR plants utilizing biogas as carbon feedstock, since the low capacity of typical biogas plants has made integration of traditional SMR's unattractive at such sites due to capacity of scale [7,10,25]. Combining the high energy efficiency with the biogenic carbon provided from biogas, an attractive solution is given for a potential competitive production of sustainable and renewable

chemicals and/or fuels with near zero carbon emission and high carbon utilization.

4. Conclusion

This study demonstrates that replacing a fired steam reformer (SMR) with an electrically heated steam methane reformer (eSMR) based on integrated electrical heating is feasible and that it provides an improved thermal response and control. The eSMR demonstrated electrical heating feedback-controlled operation from an idle state at 630 °C to operating conditions at 900 °C within 2.6 h, producing synthesis gas in thermodynamic equilibrium with respect to the reforming reactions. Additionally, the eSMR configuration enables extremely agile and stable operation for temperature changes, demonstrating heating rates in the current configurations up to 330 °C/h, where higher rates are feasible with further optimizations. With the new configuration, a high operating temperature of 1000 °C was reached with high stability and control, which is not possible in industrial SMR plants due to material constraints. This improves the methane conversion and thereby reduces the methane slip from the eSMR reactor, which will increase feed utilization. The eSMR reactor was investigated in a large operating envelope, covering 750 °C–1000 °C and 3–20 bar_g, producing syngas as expected. Better contact between the heat source and the catalyst in the eSMR reactor translates into high energy efficiency, where efficiencies of the pilot reactor were quantified between 72 % and 80 % at low capacities to provide a more comprehensive overview of the energy efficiency development. The findings were then utilized to develop a simplified energy efficiency model for the eSMR pilot plant reactor, based on its general energy balance. Extrapolating using the energy efficiency model, an energy efficiency of 99 % for the eSMR reactor was found for capacities exceeding 1 MW, this translates into an electrical energy consumption of 1.0 kWh/ Nm^3 H_2 when normalized to the syngas product in industrial steam methane reforming. A central difference between the eSMR and SMR technology is the omission of the furnace section, leading to elimination of associated flue gas of the eSMR technology. This simplifies a potential eSMR plant design markedly, since the whole furnace section is removed, including utilities within, which also increases the degree of freedom for pre-heating. Furthermore, the eSMR design allows attractive production of blue hydrogen with near complete carbon capture where the absence of the flue gas significantly decreases the energy consumption in the carbon capture process.

The eSMR plant design enables feasible operation of different reactor sizes, which promotes delocalization designs and the use of other feedstocks, including sustainable feedstocks such as biogas. The use of biogas in combination with the eSMR plant design demonstrates the possibilities of more attractive sustainable approaches for chemical plants on a large scale in the future, with practically zero-emission, high carbon utilization, and renewable electricity driven chemicals production.

Declaration of Competing Interest

The authors declare that they have no known competing financial interests or personal relationships that could have appeared to influence the work reported in this paper.

Data availability

The data that has been used is confidential.

Acknowledgment

This research is partially financed by the Energy Technology Development and Demonstration Program (EUDP) in Denmark under the project 64019-0014 entitled “eSMR-MeOH: Biogas to MeOH by electric reforming” as well as Innovation Fund Denmark (IFD) under file no. 1044-00133B. The authors greatly appreciate the biogas research facility at Aarhus University, Viborg Campus, to host and support the operation of the pilot plant. We would also like to thank the support from TOPSOE R&D for technical assistance and supports during commissioning and operation of the eSMR pilot plant.

Appendix A. Supplementary data

Supplementary data to this article can be found online at https://doi.org/10.1016/j.cej.2023.147205.

References

[1] C.o.t.E. Union, Fit for 55, 2022. https://www.consilium.europa.eu/en/policies/green-deal/fit-for-55-the-eu-plan-for-a-green-transition/. (Accessed 19/11/ 2022).
[2] UNEP-CCC, Emissions Gap Report 2020, United Nations Environment Programme, 2020, p. 128.
[3] R. Pinsky, P. Sabharwall, J. Hartvigsen, J. O’Brien, Comparative review of hydrogen production technologies for nuclear hybrid energy systems, Prog. Nucl. Energy 123 (2020), 103317, https://doi.org/10.1016/j.pnucene.2020.103317.
[4] IEA, The Future of Hydrogen, Paris, 2019.
[5] A.O. Oni, K. Anaya, T. Giwa, G. Di Lullo, A. Kumar, Comparative assessment of blue hydrogen from steam methane reforming, autothermal reforming, and natural gas decomposition technologies for natural gas-producing regions, Energ. Conver. Manage. 254 (2022), 115245, https://doi.org/10.1016/j.enconman.2022.115245.
[6] G. Lagioia, M.P. Spinelli, V. Amicarelli, Blue and green hydrogen energy to meet European Union decarbonisation objectives. An overview of perspectives and the current state of affairs, Int. J. Hydrogen Energy 48 (4) (2023) 1304–1322, https://doi.org/10.1016/j.ijhydene.2022.10.044.
[7] J. Rostrup-Nielsen, L.J. Christiansen, Concepts in syngas manufacture, Imperial College Press, 2011.
[8] R. Rapier, Estimating the Carbon Footprint of Hydrogen Production, 2020. https://www.forbes.com/sites/rrapier/2020/06/06/estimating-the-carbon-footprint-of-hydrogen-production/?sh=d09b82624bd6. (Accessed 05/12/ 2022).
[9] P.L. Spath, M.K. Mann, Life cycle assessment of hydrogen production via natural gas steam reforming, national renewable energy lab, (NREL), Golden, CO (United States) (2000).
[10] S.T. Wismann, J.S. Engbæk, S.B. Vendelbo, F.B. Bendixen, W.L. Eriksen, K. Aasberg-Petersen, C. Frandsen, I. Chorkendorff, P.M. Mortensen, Electrified methane reforming: a compact approach to greener industrial hydrogen production, Science 364 (6442) (2019) 756–759, https://doi.org/10.1126/science.aaw8775.
[11] S.T. Wismann, Electrically heated steam methane reforming, Technical University of Denmark, Lyngby, Denmark), 2019.
[12] S.T. Wismann, J.S. Engbæk, S.B. Vendelbo, W.L. Eriksen, C. Frandsen, P. M. Mortensen, I. Chorkendorff, Electrified methane reforming: elucidating transient phenomena, Chem. Eng. J. 425 (2021), 131509, https://doi.org/10.1016/j.cej.2021.131509.
[13] S.T. Wismann, J.S. Engbæk, S.B. Vendelbo, W.L. Eriksen, C. Frandsen, P. M. Mortensen, I. Chorkendorff, Electrified methane reforming: understanding the dynamic interplay, Ind. Eng. Chem. Res. 58 (51) (2019) 23380–23388, https://doi.org/10.1021/acs.iecr.9b04182.
[14] V. Palma, M. Martino, E. Meloni, A. Ricca, Novel structured catalysts configuration for intensification of steam reforming of methane, Int. J. Hydrogen Energy 42 (3) (2017) 1629–1638, https://doi.org/10.1016/j.ijhydene.2016.06.162.
[15] H.-S. Roh, D.K. Lee, K.Y. Koo, U.H. Jung, W.L. Yoon, Natural gas steam reforming for hydrogen production over metal monolith catalyst with efficient heat-transfer, Int. J. Hydrogen Energy 35 (4) (2010) 1613–1619, https://doi.org/10.1016/j.ijhydene.2009.12.051.
[16] E. Tronconi, G. Groppi, T. Boger, A. Heibel, Monolithic catalysts with ‘high conductivity’ honeycomb supports for gas/solid exothermic reactions: characterization of the heat-transfer properties, Chem. Eng. Sci. 59 (22) (2004) 4941–4949, https://doi.org/10.1016/j.ces.2004.07.018.
[17] R. Balzarotti, A. Beretta, G. Groppi, E. Tronconi, A comparison between washcoated and packed copper foams for the intensification of methane steam reforming, React. Chem. Eng. 4 (8) (2019) 1387–1392, https://doi.org/10.1039/C9RE00125E.
[18] A.Y. Tonkovich, S. Perry, Y. Wang, D. Qiu, T. LaPlante, W.A. Rogers, Microchannel process technology for compact methane steam reforming, Chem. Eng. Sci. 59 (22) (2004) 4819–4824, https://doi.org/10.1016/j.ces.2004.07.098.
[19] G. Cavusoglu, F. Dallmann, H. Lichtenberg, A. Goldbach, R. Dittmeyer, J. D. Grunwaldt, In situ characterization of catalysts and membranes in a microchannel under high-temperature water gas shift reaction conditions, J. Phys. Conf. Ser. 712 (1) (2016), 012054, https://doi.org/10.1088/1742-6596/712/1/012054.
[20] V. Balakotaiah, Z. Sun, D.H. West, Autothermal reactor design for catalytic partial oxidations, Chem. Eng. J. 374 (2019) 1403–1419, https://doi.org/10.1016/j.cej.2019.05.155.
[21] K. Aasberg-Petersen, J.H. Bak Hansen, T.S. Christensen, I. Dybkjaer, P.S. Christensen, C. Stub Nielsen, S.E.L. Winter Madsen, J.R. Rostrup-Nielsen, Technologies for large-scale gas conversion, Applied Catalysis A: General 221(1) (2001) 379-387. https://doi.org/https://doi.org/10.1016/S0926-860X(01)00811-0.

[22] L.C. Buelens, V.V. Galvita, H. Poelman, C. Detavernier, G.B. Marin, Super-dry reforming of methane intensifies CO2 utilization via Le Chatelier's principle, Science 354 (6311) (2016) 449–452, https://doi.org/10.1126/science.aah7161.
[23] K. Johnsen, H.J. Ryu, J.R. Grace, C.J. Lim, Sorption-enhanced steam reforming of methane in a fluidized bed reactor with dolomite as CO2-acceptor, Chem. Eng. Sci. 61 (4) (2006) 1195–1202, https://doi.org/10.1016/j.ces.2005.08.022.
[24] M.G. Vinum, M.R. Almind, J.S. Engbæk, S.B. Vendelbo, M.F. Hansen, C. Frandsen, J. Bendix, P.M. Mortensen, Dual-function cobalt-nickel nanoparticles tailored for high-temperature induction-heated steam methane reforming, Angew. Chem. Int. Ed. 57 (33) (2018) 10569–10573, https://doi.org/10.1002/anie.201804832.
[25] M.R. Almind, S.B. Vendelbo, M.F. Hansen, M.G. Vinum, C. Frandsen, P. M. Mortensen, J.S. Engbæk, Improving performance of induction-heated steam methane reforming, Catal. Today 342 (2020) 13–20, https://doi.org/10.1016/j.cattod.2019.05.005.
[26] P.M. Mortensen, J.S. Engbæk, S.B. Vendelbo, M.F. Hansen, M. Østberg, Direct hysteresis heating of catalytically active Ni–Co nanoparticles as steam reforming catalyst, Ind. Eng. Chem. Res. 56 (47) (2017) 14006–14013, https://doi.org/10.1021/acs.iecr.7b02331.
[27] E. Meloni, M. Martino, V. Palma, Microwave assisted steam reforming in a high efficiency catalytic reactor, Renew. Energy 197 (2022) 893–901, https://doi.org/10.1016/j.renene.2022.07.157.
[28] E. Meloni, M. Martino, A. Ricca, V. Palma, Ultracompact methane steam reforming reactor based on microwaves susceptible structured catalysts for distributed hydrogen production, Int. J. Hydrogen Energy 46 (26) (2021) 13729–13747, https://doi.org/10.1016/j.ijhydene.2020.06.299.
[29] E. Meloni, E. Saraceno, M. Martino, A. Corrado, G. Iervolino, V. Palma, SiC-based structured catalysts for a high-efficiency electrified dry reforming of methane, Renew. Energy 211 (2023) 336–346, https://doi.org/10.1016/j.renene.2023.04.082.
[30] S. Renda, M. Cortese, G. Iervolino, M. Martino, E. Meloni, V. Palma, Electrically driven SiC-based structured catalysts for intensified reforming processes, Catal. Today 383 (2022) 31–43, https://doi.org/10.1016/j.cattod.2020.11.020.
[31] P.G. Kougias, I. Angelidaki, Biogas and its opportunities—A review, Frontiers of, Environ. Sci. Eng. 12 (3) (2018) 14, https://doi.org/10.1007/s11783-018-1037-8.
[32] P.M. Mortensen, I. Dybkjær, Industrial scale experience on steam reforming of CO2-rich gas, Appl. Catal. A 495 (2015) 141–151, https://doi.org/10.1016/j.apcata.2015.02.022.
[33] K. Obaideen, M.A. Abdelkareem, T. Wilberforce, K. Elsaid, E.T. Sayed, H. M. Maghrabie, A.G. Olabi, Biogas role in achievement of the sustainable development goals: evaluation, Challenges, and Guidelines, J. Taiwan Inst. Chem. Eng. 131 (2022), 104207, https://doi.org/10.1016/j.jtice.2022.104207.
[34] P. Gupta, C. Kurien, M. Mittal, Biogas (a promising bioenergy source): A critical review on the potential of biogas as a sustainable energy source for gaseous fuelled spark ignition engines, Int. J. Hydrogen Energy (2022), https://doi.org/10.1016/j.ijhydene.2022.11.195.
[35] A. Petersson, A. Wellinger, Biogas upgrading technologies–developments and innovations, IEA Bioenergy (2009) 1–19.
[36] C. Dannesboe, J.B. Hansen, I. Johannsen, Removal of sulfur contaminants from biogas to enable direct catalytic methanation, Biomass Convers. Biorefin. 11 (5) (2021) 1823–1834, https://doi.org/10.1007/s13399-019-00570-7.
[37] C. Dannesboe, J.B. Hansen, I. Johannsen, Catalytic methanation of CO2 in biogas: experimental results from a reactor at full scale, React. Chem. Eng. 5 (1) (2020) 183–189, https://doi.org/10.1039/C9RE00351G.
[38] Iea, Outlook for biogas and biomethane: prospects for organic growth, IEA, Paris, 2020, p. 93.
[39] P. Weiland, Biogas production: current state and perspectives, Appl. Microbiol. Biotechnol. 85 (4) (2010) 849–860, https://doi.org/10.1007/s00253-009-2246-7.
[40] S.N.B. Villadsen, P.L. Fosbøl, I. Angelidaki, J.M. Woodley, L.P. Nielsen, P. Møller, The potential of biogas; the solution to energy storage, ChemSusChem 12 (10) (2019) 2147–2153, https://doi.org/10.1002/cssc.201900100.
[41] [41] A.I. Adnan, M.Y. Ong, S. Nomanbhay, K.W. Chew, P.L. Show, Technologies for Biogas Upgrading to Biomethane: A Review, Bioengineering (Basel, Switzerland) 6 (4) (2019). https://doi.org/10.3390/bioengineering6040092.
[42] K. Stangeland, D. Kalai, H. Li, Z. Yu, CO2 methanation: the effect of catalysts and reaction conditions, Energy Procedia 105 (2017) 2022–2027, https://doi.org/10.1016/j.egypro.2017.03.577.
[43] Irena, Innovation outlook: renewable methanol, international renewable energy agency, Abu Dhabi (2021) 124.
[44] R. Gaikwad, S.N. Villadsen, J.P. Rasmussen, F.B. Grumsen, L.P. Nielsen, G. Gildert, P. Møller, P.L. Fosbøl, Container-Sized CO2 to methane: design, construction and catalytic tests using raw biogas to biomethane, Catalysts 10 (12) (2020) 1428, https://doi.org/10.3390/catal10121428.
[45] S. Simon Araya, V. Liso, X. Cui, N. Li, J. Zhu, S.L. Sahlin, S.H. Jensen, M.P. Nielsen, S.K. Kær, A review of the methanol economy: the fuel cell route, Energies 13 (3) (2020) 596, https://doi.org/10.3390/en13030596.
[46] P.G. Kougias, I. Angelidaki, Biogas and its opportunities—a review, frontiers of, Environ. Sci. Eng. 12 (3) (2018) 1–12.
[47] K. Aasberg-Petersen, T.S. Christensen, I. Dybkjaer, J. Sehested, M. Østberg, R. M. Coertzen, M.J. Keyser, A.P. Steynberg, Chapter 4 - Synthesis gas production for FT synthesis, in: A. Steynberg, M. Dry (Eds.), Studies in Surface Science and Catalysis, Elsevier, 2004, pp. 258–405.
[48] S. Thor Wismann, K.E. Larsen, P. Mølgaard Mortensen, Electrical reverse shift: sustainable CO2 valorization for industrial scale, Angew. Chem. 134 (8) (2022), e202109696, https://doi.org/10.1002/ange.202109696.
[49] Topsoe, Waste Heat Boiler (Syngas). https://www.topsoe.com/our-resources/knowledge/our-products/equipment/waste-heat-boiler-syngas. (Accessed 09-01-2023).
[50] J.R. Rostrup-Nielsen, L.J. Christiansen, J.H. Bak Hansen, Activity of steam reforming catalysts: Role and assessment, Appl. Catal. 43 (2) (1988) 287–303, https://doi.org/10.1016/S0166-9834(00)82733-5.
[51] M. Nijemeisland, A.G. Dixon, E. Hugh Stitt, Catalyst design by CFD for heat transfer and reaction in steam reforming, Chem. Eng. Sci. 59 (22) (2004) 5185–5191, https://doi.org/10.1016/j.ces.2004.07.088.
[52] P. Sadooghi, R. Rauch, Experimental and modeling study of catalytic steam reforming of methane mixture with propylene in a packed bed reactor, Int. J. Heat Mass Transf. 78 (2014) 515–521, https://doi.org/10.1016/j.ijheatmasstransfer.2014.06.084.
[53] Nitrogen+ Syngas Issue 382, 2023. https://bcinsight.com//nitrogen_syngas.asp. (Accessed 17-04 2023).
[54] O. Schmidt, A. Gambhir, I. Staffell, A. Hawkes, J. Nelson, S. Few, Future cost and performance of water electrolysis: an expert elicitation study, Int. J. Hydrogen Energy 42 (52) (2017) 30470–30492, https://doi.org/10.1016/j.ijhydene.2017.10.045.